J Mol Model (2013) 19:973–983
DOI 10.1007/s00894-012-1635-5

ORIGINAL PAPER

Interaction of dihydrofolate reductase and aminoglycoside adenyltransferase enzyme from *Klebsiella pneumoniae* multidrug resistant strain DF12SA with clindamycin: a molecular modelling and docking study

Shailesh K. Shahi · Vinay K. Singh · Ashok Kumar · Sanjeev K. Gupta · Surya K. Singh

Received: 3 July 2012 / Accepted: 7 October 2012 / Published online: 25 October 2012

Abstract *Klebsiella pneumoniae* strain DF12SA (HQ114261) was isolated from diabetic foot wounds. The strain showed resistance against ampicillin, kanamycin, gentamicin, streptomycin, spectinomycin, trimethoprim, tetracycline, meropenem, amikacin, piperacillin/tazobactam, augmentin, co-trimoxazole, carbapenems, penicillins and cefoperazone, and was sensitive to clindamycin. Molecular characterization of the multidrug-resistance phenotype revealed the presence of a class 1 integron containing two genes, a dihydrofolate reductase (*DHFR*) (PF00186), which confers resistance to trimethoprim; and aminoglycoside adenyltransferase (*AadA*) (PF01909), which confers resistance to streptomycin and spectinomycin. A class 1 integron in *K. pneumoniae* containing these two genes was present in eight (18.18 %) out of 44 different diabetic foot ulcer (DFU) patients. Hence, there is a need to develop therapeutics that inhibit growth of multidrug resistant *K. pneumoniae* in DFU patients and still achieve amputation control. Am attempt was made to create a 3D model and find a suitable inhibitor using an in silico study. Rational drug design/testing requires crystal structures for DHFR and AadA. However, the structures of DHFR and AadA from *K. pneumoniae* are not available. Modelling was performed using Swiss Model Server and Discovery Studio 3.1. The PDBSum server was used to check stereo chemical properties using Ramachandran plot analysis of modeled structures. Clindamycin was found to be suitable inhibitor of DHFR and AadA. A DockingServer based on Autodock & Mopac was used for docking calculations. The amino acid residues Ser^{32}, Ile^{46}, Glu^{53}, Gln^{54}, Phe^{57}, Thr^{72}, Met^{76}, Val^{78}, Leu^{79}, Ser^{122}, Tyr^{128}, Ile^{151} in case of DHFR and Phe^{34}, Asp^{60}, Arg^{63}, Gln^{64}, Leu^{68}, Glu^{87}, Thr^{89}, Val^{90} for AadA were found to be responsible for positioning clindamycin into the active site. The study identifies amino acid residues crucial to 'DHFR and AadA -drug' and 'DHFR and AadA -inhibitor' interactions that might be useful in the ongoing search for a versatile DHFR and AadA -inhibitor.

Keywords Antibiotic resistance · Integrons · *Klebsiella pneumoniae* · Homology search · Dihydrofolate reductase · Aminoglycoside adenyltransferase

Electronic supplementary material The online version of this article (doi:10.1007/s00894-012-1635-5) contains supplementary material, which is available to authorized users.

S. K. Shahi · V. K. Singh · A. Kumar (✉)
School of Biotechnology, Faculty of Science,
Banaras Hindu University,
Varanasi 221005, India
e-mail: kasokbt@rediffmail.com

S. K. Gupta
Department of General Surgery, Institute of Medical Sciences,
Banaras Hindu University,
Varanasi 221005, India

S. K. Singh
Department of Endocrinology and Metabolism,
Institute of Medical Sciences, Banaras Hindu University,
Varanasi 221005, India

Introduction

Diabetic foot ulcer (DFU) and infections are a major medical, social, economic problem and a leading cause of morbidity and mortality, especially in developing countries like India [1]. Sporadic qualitative research suggests that diabetic foot ulceration has a profound social impact, with patients reporting stigma, social isolation, loss of social role, and unemployment [2]. DFU is highly susceptible to infection, which can spread rapidly, leading to overwhelming tissue destruction

and subsequent amputation [3]. Results from studies of microbiological cultures from DFUs have indicated that the most frequently identified isolates are aerobes including *Staphylococcus aureus*, *Staphylococcus epidermidis*, coagulase-negative *Staphylococcus* spp., *Enterococcus* spp., *Escherichia coli*, *Pseudomonas aeruginosa*, *Proteus mirabilis* and *K. pneumoniae* (*Klebsiella pneumoniae*) [4], with *K. pneumoniae* being the most common aetiological agent in diabetic foot infection [5]. *K. pneumoniae* is a Gram-negative, non-motile, rod-shaped bacterium also known as an opportunistic pathogen found in the environment and in mammalian mucosal surfaces. Generally, *K. pneumoniae* infections tend to occur in patients with a weakened immune system and people with underlying diseases [6].

The incidence of multi drug resistance (MDR) *K. pneumoniae* infection in DFU has become a serious problem worldwide. Umadevi et al. [5] isolated 20.5 %*K. pneumoniae* from DFU patients in south India. Most of the isolated *K. pneumoniae* strains were susceptible to amikacin, piperacillin-tazobactam and imipenem, but resistant to tetracycline, ciprofloxacin, trimethoprim-sulfamethoxazole, gentamicin, netilmicin, cefuroxime, ceftriaxone, ceftazidime, and imipenem except amoxicillin-clavulanic acid, to which they showed variable susceptibility [5]. In the last two decades, MDR phenotypes have spread widely among Gram-negative bacteria. The spread of MDR among Gram-negative bacteria is due mainly to the presence of class 1 integrons [7]. Mobile genetic elements such as plasmids, transposons and integrons are able to facilitate antibiotic resistance by spread of genetic material between species or genera of bacteria. Integrons are classified according to integrase sequence [8]. To date, five classes of integrons (classes 1, 2, 3 4, 5) have been reported to be associated with the resistance gene cassettes [9]. Class 1 integrons are found most frequently among multi-resistant *Klebsiella* sp. [10]. Class 1 integrons are associated with a variety of resistance gene cassettes, but most integrons contain dihydrofolate reductase (DHFR), which confers resistance to trimethoprim; and an aminoglycoside adenyltransferase gene, which confers resistance to streptomycin and spectinomycin [8]. DHFR is a central enzyme in the folate biosynthetic pathway of both prokaryotic and eukaryotic cells, and is also encoded by several viral genomes. DHFR plays a key role in maintaining intracellular folate homeostasis, cell growth and proliferation, and is an important target for cytostatic drugs [11]. As a result of its obvious clinical importance, it has been studied extensively using a wide range of experimental and theoretical methods [12]. As a drug target against bacterial, fungal and protozoan infections and for treatment of rheumatological diseases and cancer, DHFR is of fundamental pharmaceutical importance [13]. Bacterial resistance to aminoglycosides protects itself by aminoglycoside-modifying enzymes such as aminoglycoside adenyltransferase (AadA), aminoglycoside acetyltransferases (AACs) and aminoglycoside phosphotransferases (APHs), which inactivate them, decreased cell membrane permeability towards aminoglycoside uptake into the cell, structural alteration in the ribosomal target of the drug and/or extrusion of the aminoglycosides from the cell by efflux pumps. A number of bacteria also harbor a unique bifunctional resistance enzyme that catalyzes both the AAC and APH reactions [14, 15]. Aminoglycoside modifying enzymes are the most important mechanism both in terms of level and frequency of resistance conferred to the bacterium. Considering the pharmaceutical importance of DHFR and AadA and a possible drug target in MDR bacteria, various in silico approaches have been applied to the study of their structural and functional properties.

In this work, we obtained the sequence of DHFR and AadA from *K. pneumoniae* strain DF12SA and predicted its structure by homology modeling. Identification of the amino acid residues crucial to the interaction between DHFR and AadA (the enzymes produced by resistant bacteria) with clindamycin (the drug not hydrolyzed by this bacterial enzyme) was also performed. This information might be useful to scientists involved in drug-design in their search for more potent and versatile DHFR and AadA inhibitors. Comparative modeling is a useful tool in bioinformatics to predict the three dimensional (3D) structure of an unknown protein. It is an invaluable aid to understand protein function and also a preliminary step towards establishing it as a promising drug target in *K. pneumoniae*. Docking studies between DHFR and AadA with its potential antibiotic inhibitor clindamycin were also performed.

Materials and methods

Patients, sample collection and isolation of bacteria

This study was conducted in the Department of Endocrinology and Metabolism, and Department of General Surgery, Sir Sunderlal Hospital, Institute of Medical Sciences, in collaboration with the School of Biotechnology, Banaras Hindu University, Varanasi. The study was conducted after seeking prior approval of the ethical committee of the Institute (Ref. No. Dean/2009-10/555 dated 11 July 11 2009). In total, 44 severe DFU patients (grades III–V) attending to the hospital between January 2010 and October 2011 were selected for this study. Prior written consent was obtained from every recruited patient. DFUs, i.e., grade 0- hyperkeratosis; grade 1-superficial ulcers; grade 2-deep ulcers; grade 3-tendonitis, osteomyelitis, cellulites, or abscess; grade 4-gangrene of a toe or forefoot; and grade 5-massive gangrene of the whole foot were graded according to Wagner [16]. Two biopsy samples from the ulcer of the diabetic foot of each patient were taken using a sterilized punch biopsy needle (6 mm) under local anesthesia. Wound

biopsies were collected from the foot ulcer of the patients under aseptic conditions. Debridement was done with meticulous care to eliminate the colonizing bacteria from the site. Two swab samples were collected by washing the wound with sterile physiological saline and then by applying a sterile cotton swab to the wound. Of two biopsy and swab samples, one was used for detecting *K. pneumoniae* through in vitro culture, the second for performing *K. pneumoniae*-specific 16S rDNA (ribosomal DNA) amplification. For in vitro culture each sample (swab and biopsy) was plated directly on different aerobic growth media such as MacConkey agar, and chocolate agar and the plates were incubated at 35 °C in an incubator. Biopsy samples were gently macerated before inoculation. The plates were examined after 24–36 h of incubation and distinct colonies appearing on each plate were picked up and restreaked on the corresponding medium. Tentative identification of *K. pneumoniae* isolates was made on the basis of Gram's staining and morphological characters as well as biochemical tests namely, catalase, nitrate reductase, urease, Simmons citrate utilization and MR (methyl red) using standard methods.

Amplification of *Klebsiella pneumoniae*-specific 16S rDNA

Genomic DNA was extracted using a DNeasy Tissue Kit (Qiagen, Hilden, Germany) as per the manufacturer's instructions. The 16S rDNA (1,361 bp) of laboratory-grown pure cultures was amplified using *K. pneumoniae* primers, viz. Fd. 5′-ACTCCCGATCCCTGAGCCCTTTTC-3′ and Rev. 5′-GGTCAGAGCAGGCG TTT CCA CC-3′. Amplification was performed in a PTC-100 Thermal Cycler (MJ Research, Waltham, MA). The PCR reaction mix included 1.5 U *Taq* DNA polymerase (Bangalore Genei, Bangalore, India), 1× PCR buffer with 1.5 mmol/L $MgCl_2$ (1 mmol/L $MgCl_2$ was added so as to attain a final concentration of 2.5 mmol/L), 25 pmol each of the forward and reverse primers (Integrated DNA Technologies, Coralville, IA), 125 μmol/L each of the dNTPs (deoxynucleotide triphosphates), and 50 ng template DNA in a total volume of 50 μL. Thermal cycles for the amplification were set at initial denaturation for 10 min at 94 °C, 30 cycles of 40s at 94 °C, 40s at 60 °C, and 1 min at 72 °C, followed by a final extension of 7 min at 72 °C. The amplified product (1,361 bp) was visualized on 1.2 % agarose gel using a gel documentation unit (BioRad, Hercules, CA).

Antimicrobial susceptibility testing

Antimicrobial susceptibility test of cultured *K. pneumoniae* was done by the disc diffusion method using the Kirby-Bauer method [17]. A total of 16 antibiotics [spectinomycin (100 μg), streptomycin (20 μg), trimethoprim (20 μg), gentamicin (10 μg), ampicillin (10 μg), tetracycline (30 μg), kanamycin (30 μg), amikacin (30 μg), augmentin (30 μg), cefoperazone (75 μg) meropenem (10 μg), Piperacillin/tazobactam (100/10 μg), co-trimoxazole (1.25/23.75 μg), penicillins (10 μg), carbapenems (2 μg) and clindamycin (2 μg)] was selected according to published recommendations and their widespread use in treatment of various diseases [1]. Ampicillin, augmentin and clindamycin are penicillins, spectinomycin, streptomycin, gentamicin, kanamycin and amikacin are aminoglycosides, tetracycline belongs to tetracycline class, meropenem is a carbapenems, cefoperazone is a cephalosporin, and trimethoprim belongs to the class of chemotherapeutic agents (DHFR inhibitor). Co-trimoxazole is a folate pathway inhibitor. Piperacillin/tazobactam are β-lactam antibiotics. The disks were purchased from Micro Master Laboratories (Mumbai, India). Interpretation of results was based on Clinical and Laboratory Standards Institute (CLSI) guidelines 2007 [18]. Antibiotic susceptibity, intermediate susceptibility or resistance was assessed by measuring the diameter (mm) of the clear zone around the disc.

Amplification of class 1 integron

Genomic DNA was extracted using a DNeasy Tissue Kit (Qiagen) following the manufacturer's instructions. The class 1 integron (1,580 bp) was amplified using primers 5′-CS-5′-GGC ATC CAA GCA GCA AG-3′ and 3′CS-5′-AAG CAG ACT TGA CCT GA-3′ in a PTC-100 Thermal Cycler (MJ Research) [19]. The reaction was performed in a final volume of 50 mL, which included 1.5 U *Taq* DNA polymerase, 1×*Taq* assay buffer containing 1.5 mM $MgCl_2$, 125 mM each dNTPs (Bangalore Genei), 50 pmol of each primers (Integrated DNA Technologies) and 100 ng template DNA. Thermal cycles for the amplification were set at initial denaturation of 7 min at 94 °C, 35 cycles of 1 min denaturation at 94 °C, 1 min annealing at 59 °C, 2 min 30 s of extension at 72 °C followed by 7 min of final extension at 72 °C. The reaction products of PCR were subjected to electrophoresis in a 1.0 % agarose gel, stained with ethidium bromide and visualized under UV light in gel documentation unit (Bio-Rad). *K. pneumoniae* ATCC 700603 was used as a control strain.

Restriction digestion of amplified class 1 integron

The class 1 integron (1.58 kb) amplified from *K. pneumoniae* isolates viz. DF6SB, DF11SB, DF12SA, DF13TA, DF14TA, DF29TC, DF38TB and DF41TC was purified and subjected to digestion by *Alu*I and *Rsa*I restriction endonuclease according to the instructions of manufacturer (New England Biolabs, Hitchin, UK). Restriction digestion was done in a final volume of 25 μL containing 1 X restriction enzyme buffer, 0.30 μL (3.0 U) restriction enzyme and 15 μL PCR products. After mixing, samples were incubated for 6 h in a water bath preset at 37 °C. Reaction was terminated by heat inactivation of restriction enzymes at 70 °C for 20 min . The samples were

analyzed by agarose gel (3 %) electrophoresis and monitored on gel documentation unit (Bio-Rad).

Sequencing and deposition of class 1 integron

The PCR fragment was purified from the agarose gel using a QIA quick gel extraction kit (Qiagen). The PCR products were sequenced from Chromous Biotech (Bangalore, India). After complete annotation sequence was deposited in National Center for Biotechnology Information (NCBI, http://www.ncbi.nlm.nih.gov/).

Gene annotation and similarity search

Sequences from PCR amplification from *K. pneumoniae* strain DF12SA were used in an ORF scan (http://www.ncbi.nlm.nih.gov/gorf/gorf.html) to identify coding regions (exons) in amplified sequences. FGENESB was used to find the presence of bacterial operons and genes in raw sequence [20]. The predicted protein sequences were subjected to protein functional analysis using INTERPROSCAN version 4.4 [21]. These sequences of both proteins from different species were aligned using ClustalW [22] and a phylogenetic tree was constructed using the UPGMA method. A tree was inferred by bootstrap phylogenetic inference using MEGA3.1 [23]. The conserved motifs present in these sequences were analyzed using BLOCKS and MEME (multiple EM for motif elicitation) software version 3.5.7 [24, 25]. For motif analysis of both domain of predicted proteins, the selection of maximum number of motifs was set to 20 with minimum width of 100 amino acids, while for genes a maximum number of motifs was set to 300 while other factors were default selections. These selections were made in order to minimize the 'E-value' of the given parameter based on the probability of finding an equally well conserved pattern in a set of sequences.

Retrieval of the target protein sequence and template identification

Predicted genes and proteins sequence of DHFR and AadA from Gene cassette (HQ114261) were used as targets for homology modeling. Swiss model and Discovery studio 3.1 [26–28] were used for comparative homology modeling of DHFR and AadA from *K. pneumoniae* strain DF12SA using template structures. PDB advance BLAST (http://www.rcsb.org/pdb/home/home.do) was applied for template identification to construct 3D models of the target proteins using homology modeling.

Model refinement and evaluation

Successfully predicted 3D models of DHFR and AadA were used for refinement and evaluation. The rough generated model was subjected to energy minimization using the steepest descent technique to eliminate bad contacts between protein atoms. Computations were carried out in vacuo with the GROMOS96 43B1 parameters set, implemented through Swiss-Pdb Viewer (http://expasy.org/spdbv/). The backbone conformation of the rough model was inspected using the Phi/Psi Ramachandran plot of PDBSum Database (http://www.ebi.ac.uk/pdbsum/) [29] and Discovery Studio 3.1 (Accelrys). The BLAST2Seq server (http://blast.ncbi.nlm.nih.gov/Blast.cgi) was employed to perform alignment between the target and template sequence. ProSA server (https://prosa.services.came.sbg.ac.at/prosa.php) was used to check the model quality. After refinement evaluated model was deposited successfully with Protein Model DataBase (PMDB; http://mi.caspur.it/PMDB/).

Superimposition of target and template

The structural superimposition of C^{α} trace of the templates (3IX9 and 2RFF) and predicted model of DHFR and AadA was performed using the quaternion eigenvalue approach (http://wishart.biology.ualberta.ca/SuperPose/) [30] and combinatorial extension method (http://cl.sdsc.edu/ce/ce_align.html).

Active site prediction and docking

After obtaining the final model, the possible binding sites of DHFR and AadA were searched using Q-SiteFinder (http://bmbpcu36.leeds.ac.uk/qsitefinder/).Ten binding sites were obtained for DHFR and AadA using Q-SiteFinder. These binding sites were compared to the active site of the template to determine residues forming the binding pocket. Based on previous studies in other micro-organisms, the effect of antibiotic clindamycin $C_{18}H_{33}ClN_2O_5S$ {(2S,4R)-N-[2-chloro-1-[(2R,3R,4S,5R,6R)-3,4,5-trihydroxy-6-methylsulfanyloxan-2-yl]propyl]-1-methyl-4-propylpyrrolidine-2-carboxamide)} was found to inhibit DHFR and AadA. This inhibitor was docked successfully with DHFR and AadA using Autodock & Mopac based dockingServer http://www.dockingserver.com/web [31]. Docking calculations were carried out using DockingServer. Docking simulations were performed using the Lamarckian genetic algorithm and the Solis & Wets local search method [32]. Gasteiger partial charges were added to the ligand atoms. Each docking experiment was derived from ten different runs that were set to terminate after a maximum of 250,000 energy evaluations. The population size was set to 150. During the search, a translational step of 0.2 Å, and quaternion and torsion steps of 5 were applied. The ligand is flexible to their single bonds. DockingServer identify the rotatable bonds, which were allowed to rotate freely during the docking runs. Whole proteins were treated as rigid molecules. Essential hydrogen

atoms, Kollman united atom type charges, and solvation parameters were added with the aid of AutoDock tools [33]. AutoDock parameter was set as default.

Results and discussion

Isolation and identification of *K. pneumoniae*

K. pneumoniae was isolated successfully from biopsy/swab samples of 8 (18.18 %) out of 44 patients in Varanasi. A study from south India reported that 20.5 % of diabetic foot patients are infected with *K. pneumoniae* [5]. Isolates of *K. pneumoniae* were identified on the basis of morphological characters, biochemical tests and amplification of the *K. pneumoniae*-specific 16S rDNA. All the strains showed amplification of the desired fragment of 16S rDNA (1,361 bp) with *K. pneumoniae* species-specific primers. DNA isolated from the biopsy/swab was used as the template for direct diagnosis of *K. pneumoniae*. The expected amplicon was found in 5 biopsy and 3 swab samples out of 44 (result not shown). That these strains indeed belong to *K. pneumoniae* was further confirmed by sequencing of the class 1 integron of selected strains of *K. pneumoniae*. The sequences showed 99 % homology with sequences available for *K. pneumoniae* (accession no. FJ876827) in the NCBI database. Newly annotated sequence was deposited with NCBI under accession no. HQ114261.

Antibiotic sensitivity test

Antibiotic sensitivity tests revealed that *K. pneumoniae* strain DF12SA was resistant to ampicillin, kanamycin, gentamicin, streptomycin, spectinomycin, trimethoprim, tetracycline, meropenem, amikacin, piperacillin+tazobactam, augmentin, co-trimoxazole, carbapenems, penicillins and cefoperazone, but sensitive to clindamycin. The results of antibiotic sensitivity assays of *K. pneumoniae* isolates, viz. DF6SB, DF11SB, DF12SA, DF13TA, DF14TA, DF29TC, DF38TB and DF41TC are listed in Table 1. Interestingly, all the strains tested were found to be resistant to penicillin, streptomycin, spectinomycin, trimethoprim and co-trimoxazole. The presence of same gene cassette of class 1 integron may be the reason for the similar resistance phenotype. The high resistance recorded by *K. pneumoniae* against several antibiotics in the present study could be attributed to the uncontrolled consumption of antibiotics by diabetic foot patients.

Gene cassettes of the class 1 integron from *K. pneumoniae* strain DF12SA

The spread of MDR among Gram-negative bacteria is due mainly to the presence of class 1 integrons [7]. The growing rate of resistance of *K. pneumoniae* has thrown up the additional challenge of effectively managing disease and infections associated with this organism. In order to assess the relationship between the resistance phenotype of *K. pneumoniae strain* DF12SA and the presence of the class 1 integron, the strain was tested using PCR. PCR amplicon (1,580 bp) was uniformly observed in all strain of *K. pneumoniae* (Fig. 1a). DNA sequencing of the class 1 integron identified two ORFs. The first encodes a *DHFR*, which confers resistance to trimethoprim; and the second encodes *AadA*, which confers resistance to streptomycin and spectinomycin. A similar sized amplicon obtained from amplification of class 1 integron was subjected to restriction digestion by *Alu*I and *Rsa*I. The *Alu*I digestion pattern of *K. pneumoniae* viz. DF6SB, DF11SB, DF12SA, DF13TA, DF14TA, DF29TC, DF38TB and DF41TC are shown in Fig. 1b. The same pattern among isolates was obtained upon *Rsa*1 digestion of the 1,580 bp product (results not shown). It was observed that the class 1 integron of *K. pneumoniae* isolated from different diabetic foot infected patients contained the same gene cassettes (*DHFR* and *AadA*). The relationship between the resistance phenotype to number of antibiotic viz. ampicillin, kanamycin, gentamicin, tetracycline, meropenem, amikacin, piperacillin/tazobactam, augmentin, co-trimoxazole, carbapenems, penicillins and cefoperazone may be due to three reasons: first, production of extended spectrum β-lactamases, i.e., AmpC β-lactamases that destroy the antibacterial agent before it can have an effect. Second, resistance may acquire efflux pumps that extrude the antibacterial agent from the cell before it can reach its target site and exert its effect. Third, the bacteria may have acquired several genes for a metabolic pathway that ultimately produces altered bacterial cell walls that no longer contain the binding site for the antimicrobial agent, or the bacteria may have acquired mutations that limit access of antimicrobial agents to the intracellular target site via downregulation of porin genes [34].

Gene annotation and similarity search

Approximately 1,580 bp sequence of the class 1 integron for multidrug resistance in *K. pneumoniae* strain DF12SA was used for in silico analysis. A search for ORFs in the amplified fragment showed eight exons in six reading frames, and INTERPROSCAN analysis of each exon suggests that two of these exons are playing an important role. The two exons showed similarity with the dfr17 (PF00186) and aadA5 (PF01909) protein family (Supplementary file 1). Two ORFs also seemed to encode full length genes using a gene prediction (FgeneshB) tool. The annotated exons are assigned protein IDs ADV78524.1 and ADV78525.1 for DHFR and AadA, respectively. These two identified proteins were used in a BLAST (basic local alignment search tool) search to find homologous regions in different bacterial species sequences existing in the biological database (NCBI). Multiple sequence

Table 1 Sensitivities of *Klebsiella pneumonia* strains to different classes of antibiotic. *R* Resistant, *S* Sensitive

Antimicrobial class	Agent	DF6SB	DF11SB	DF12SA	DF13TA	DF14TA	DF29TC	DF38TB	DF41TC
Aminoglycosides	Ampicillin	R	R	R	R	R	R	S	R
	Augmentin	S	S	R	R	S	S	S	S
	Clindamycin	S	S	S	S	R	S	S	S
	Penicillins	R	R	R	R	R	R	R	R
	Spectinomycin	R	R	R	R	R	R	R	R
	Streptomycin	R	R	R	R	R	R	R	R
	Gentamicin,	R	R	R	R	R	R	S	R
	Kanamycin	R	R	R	R	R	R	R	S
	Amikacin	S	S	R	S	S	S	R	R
Tetracyclines	Tetracycline	R	R	R	R	R	R	R	R
Cephalosporin	Meropenem	R	R	R	R	R	R	R	R
	Carbapenems	S	S	R	S	R	R	R	S
	Cefoperazone	S	S	R	S	R	S	S	S
Dihydrofolate reductase inhibitor	Trimethoprim	R	R	R	R	R	R	R	R
Folate pathway inhibitor	Co-trimoxazole	R	R	R	R	R	R	R	R
β-lactam antibiotics	Piperacillin/tazobactam	S	S	R	R	S	R	R	S

alignment revealed highly conserved regions in both the *DHFR* and *AadA* genes (Supplementary files 2 and 3). Phylogenetic analysis among different species shows two clusters in which the closest neighbors in the *DHFR* gene tree are in *Escherichia coli* and *Enterobacter cloacae* (Supplementary file 4a). *AadA* gene alignments indicate a multilevel consensus sequence against different organisms, viz. *Riemerella anatipestifer*, *Kluyvera intermedia*, *Vibrio cholerae*, *E. coli* and *Achromo bacterxylosoxidans* while *DHFR* gene alignments reveal a multilevel consensus sequence with different organisms, viz. *Salmonella enterica*, *Serratia sp*. *E. coli* and *Enterobacter cloacae* (Supplementary file 4b). One multilevel consensus motif is present in DHFR and two conserved motifs are observed in AadA protein sequence (Fig. 2).

Homology modeling of both proteins of *K. pneumoniae*

The absence of a 3D structure for *K. pneumoniae* DHFR and AadA protein in PDB prompted us to construct a 3D model (Fig. 3a, b). The 3D structure provides valuable insight into molecular function and the interactions with suitable inhibitors. The model structures of DHFR and AadA from *K.*

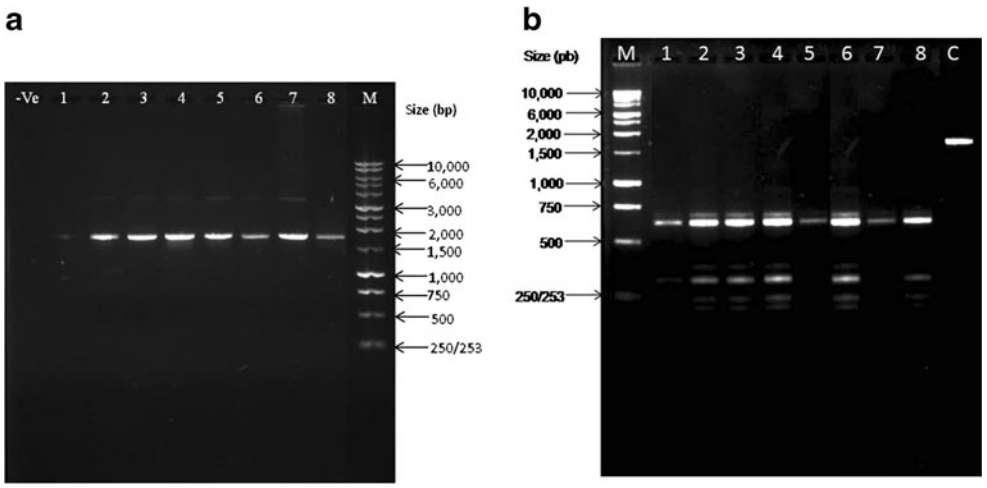

Fig. 1 **a** PCR amplification of aminoglycoside adenyltransferase/dihydrofolate reductase (*AadA*/*DHFR*) genes from different antibiotic resistant bacteria using primers 5′CS-3′CS. Lanes: *1* DF12SA; *2* DF6SB; *3* DF13TA; *4* DF14TA; *5* DF29TC; *6* DF41TC; *7* DF38TB; *8* DF11SB; *M* 1,000 bp ladder (Promega, Madison, WI). **b** Typical representation of *Alu*1 digestion pattern of 1.85 kb class integron of various *Klebsiella pneumoniae* strains. Lanes: *1–8* As in **a**, *C* undigested amplicon

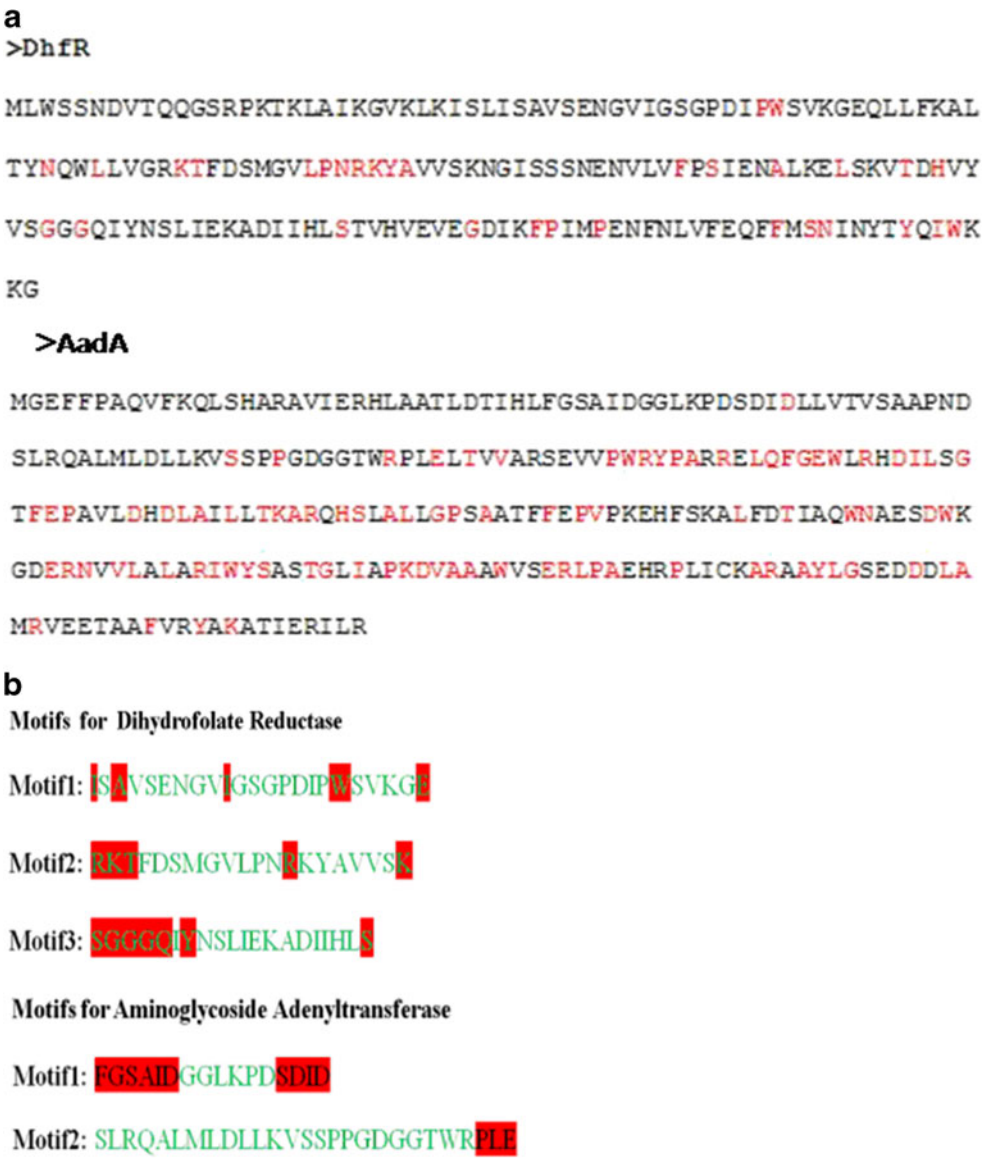

Fig. 2 **a** Sequence conservation of DHFR and AadA represented in *red*. **b** Active site residues of identified motifs of DHFR and AadA highlighted in *red*

pneumoniae strain DF12SA consists of two functional domains at the interface at which catalysis occurs. To construct the 3D model of DHFR and AadA, PDB BLAST was used for template identification. PDB BLAST analysis revealed that *K. pneumoniae* DHFR shares 34 % identities and 52 % positivity with *Streptococcus pneumoniae* and, in case of *K. pneumoniae* AadA 30 % identities and 56 % positivity with the known *Sulfolobus solfataricus* crystal structure. Accordingly, the *Streptococcus pneumoniae* DHFR crystal structure (3IX9.pdb) was used as a suitable template for *K. pneumoniae* DHFR [35]. *Sulfolobus solfataricus* crystal structure (2RFF.pdb) was used as a suitable template for *K. pneumoniae* AadA based on homology modeling [36]. Since *K. pneumoniae* DHFR and AadA protein sequence are structurally closely similar to *Streptococcus pneumoniae* and *Sulfolobus solfataricus*, respectively, at the secondary structure level as well as belonging to their respective families, the *Streptococcus pneumoniae* and *Sulfolobus solfataricus* structures were considered for 3D prediction for both sequences. DS Modeler of Discovery studio 3.1 software and the Swiss Model Server were used for homology modeling. The 3D structures of *K. pneumoniae* DHFR and AadA were constructed successfully with best molecular modeling parameter.

Validation of the predicted structure

The stereochemistry of the constructed models of DHFR and AadA was subjected to energy minimization and the stereochemical quality of the predicted structure was assessed. The Ramachandran plot for the DHFR model showed 96.6 % of residues in the core region, 83.5 % of residues in the allowed regions and 13.1 % in additional allowed regions; one residue (Ser^{95}) was in the disallowed region and present in the loop region of secondary structure. This residue (Ser^{95}) was

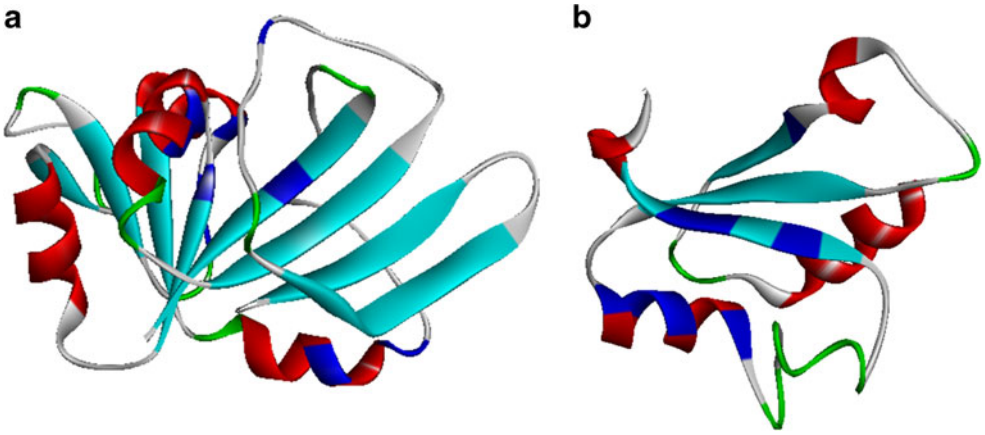

Fig. 3 Predicted three-dimensional (3D) models secondary elements: *red* α-helices, *cyan* β-sheets, *green* turns, *white* coils. The most conserved active site residues shown in *blue*. **a** Dihydrofolate reductase (DHFR). **b** Aminoglycoside adenyltransferase (AadA)

subjected to loop refinement and further energy minimization. In an analysis of the final model, 97.0 % of the residues were found to occupy the core region. The residue in the disallowed region had been shifted to the generously allowed region, thereby optimizing and stabilizing the overall conformation of the predicted structure. In the AadA model, there were 97.3 % of the residues in the core region, 82.4 % residues in the allowed regions and 14.9 % in additional allowed regions, and no residues in the disallowed region, thereby optimizing and stabilizing the overall conformation of the predicted AadA structure (Supplementary file 5a). The best refined and validated structures were deposited with the PMDB database under PMDB ID PM0078153 and PM0078154, respectively.

Superimposition of the template with predicted structure

The weighted root mean square deviation (RMSD) of the C^{α} trace between the template and the final refined model of DHFR was 0.6 Å, with a significant *Z*-score of 7.6, for AadA the RMSD was 0.8 Å with a significant *Z*-score of 4.9. SuperPose server results revealed that RMSD of the backbone trace between the template and DHFR model was 9.63 Å. Superimposition between template and AadA model revealed 19.36 Å RMSD at backbone level.

Active site identification in DHFR and AadA

Among the ten binding sites obtained from Q-Site finder (Fig. 4), site 1 is highly conserved with the active site of both templates. The results of multiple sequence alignment and secondary structure prediction revealed that the residues in site 1 (Ile^{31}, Ser^{32}, Ala^{33}, Ile^{40}, Gly^{41}, Ser^{42}, Pro^{44}, Asp^{45}, Ile^{46}, Trp^{48}, Glu^{53}, Gln^{54}, Leu^{55}, Phe^{57}, Lys^{58}, Gly^{69}, Arg^{70}, Lys^{71}, Thr^{72}, Ser^{75}, Met^{76}, Leu^{79}, Pro^{80}, Arg^{82}, Val^{87}, Ser^{88}, Lys^{89}, $^{122}SGGGQIY^{128}$ and Ile^{151}) in the active site of the template are conserved (Fig. 4a). The binding pocket of *K. pneumoniae* DHFR with clindamycin was also compared to reported *E. coli* DHFR active sites (2D0K, 3DAU, 1DDS). The binding pocket containing the Leu^{79}, Pro^{80}, Arg^{82}, Val^{87}, Ser^{88}, Lys^{89}, $^{122}SGGGQIY^{128}$ and Ile^{151} residues was conserved and therefore considered for docking analysis. In case of AadA site 1, Asn^{59}, Asp^{60}, Arg^{63}, Gln^{64}, Met^{67}, Leu^{68}, Ser^{75}, Pro^{76}, Pro^{77}, Glu^{87}, Leu^{88} and Thr^{89} are conserved with the active site of the template (Fig. 4b). The binding pocket of *K. pneumoniae* AadA with clindamycin was compared to reported active sites of *Sulfolobus solfataricus* AadA. Thus, in both cases site 1 was chosen in this study as the most favorable active binding sites for docking studies and the other sites are not discussed further.

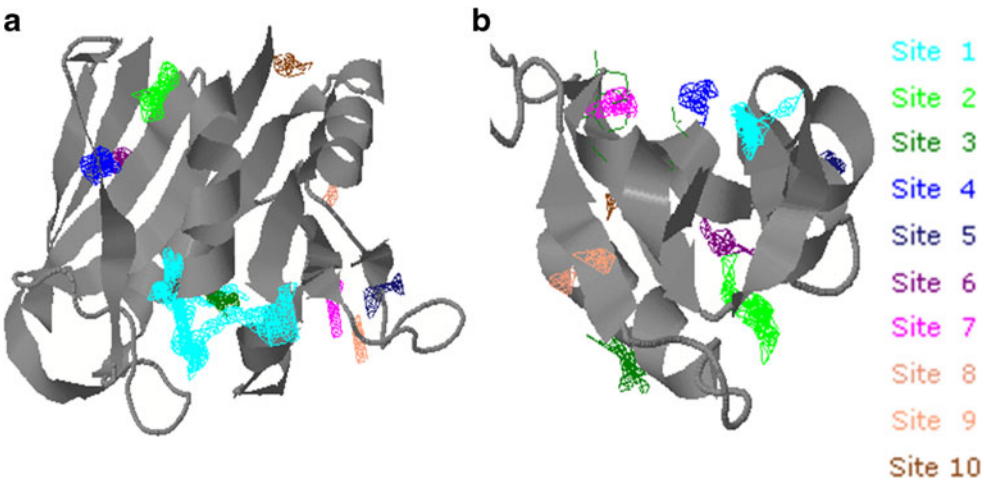

Fig. 4 Active site identification of (**a**) DHFR and (**b**) AadA using Q-site finder

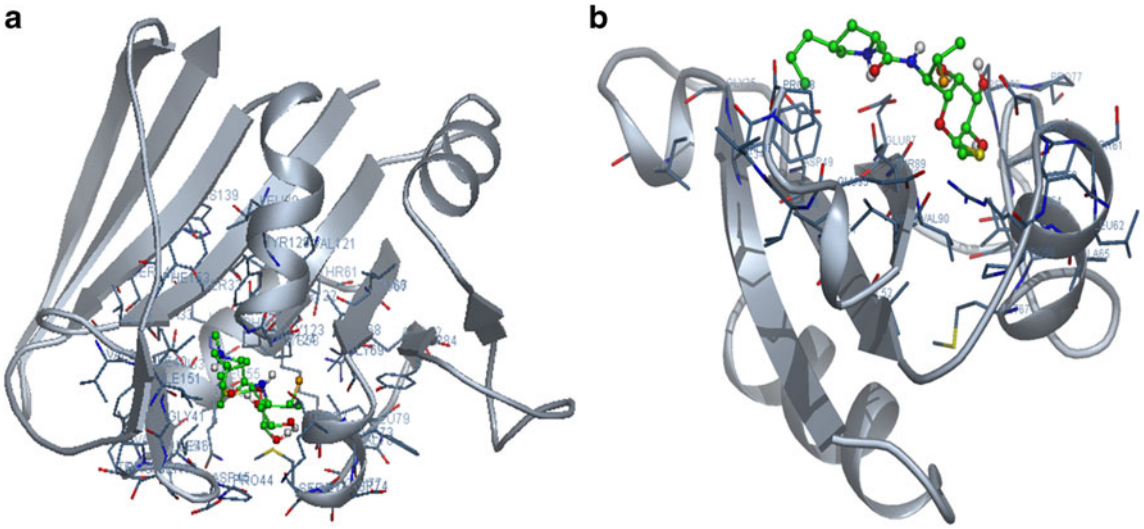

Fig. 5 Docking studies of **a** DHFR and **b** AadA with clindamycin

The DHFR and AadA in *Streptococcus pneumoniae* and *Sulfolobus solfataricus* with *K. pneumoniae* adopt a similar α/β fold but are quite distinct at the active site regions. Thus, based on our results from sequence analysis, molecular modeling and docking, we infer that the 3D structures of *K. pneumoniae* DHFR and AadA contains important catalytic active site residues that are responsible for inhibitory activity with clindamycin and show similarity with the template DHFR and AadA from *Streptococcus pneumoniae* and *Sulfolobus solfataricus*, respectively. The crystal structure of DHFR from *Streptococcus pneumoniae*, determined at 1.95 Å resolution, revealed that each monomer consists of two α/β fold domains, a unique structure that has not been observed in others. The structure of AadA from *Sulfolobus solfataricus*, determined at 1.40 Å resolution, revealed that each monomer consists of two α/β fold domains (Supplementary file 5b).

Docking with potential inhibitor

Docking of DHFR and AadA was performed with an inhibitor compound, namely clindamycin {(2S, 4R)-N-[2-chloro-1-[(2R, 3R, 4S, 5R, 6R)-3, 4, 5-trihydroxy-6-methylsulfanyloxan-2-yl] propyl]-1-methyl-4-propylpyrrolidine-2-carboxamide)} (Fig. 5). The final docked conformations obtained for this inhibitor were evaluated based on the number of hydrogen bonds formed and the bond distance between atomic co-ordinates of the active site and inhibitor. To evaluate the structural similarity of *K. pneumoniae* DHFR and AadA with related bacterial species, we performed a multiple sequence alignment of *K. pneumoniae* DHFR and AadA with the DHFR and AadA of different species. Based on the results of DHFR multiple alignment, we observe that the LPNRKYA are highly conserved across species, and that residues Pro[47],Trp[48], Asn[63], Leu[66], Lys[71], Thr[72], Phe[102], Ser[104], Ala[108], Leu[112], Thr[116], His[118], Gly[123],

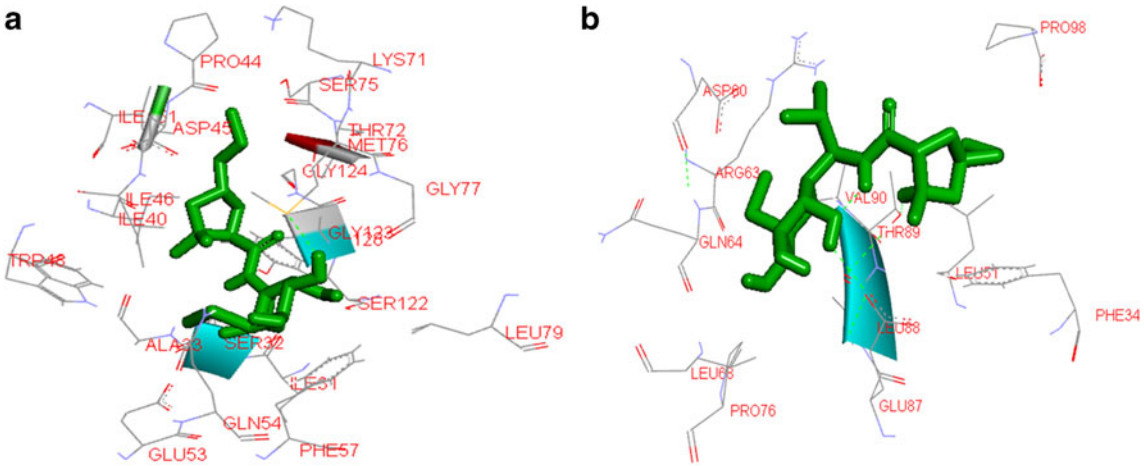

Fig. 6 Residues of **a** DHFR and **b** AadA interacting with clindamycin

Gly^{125}, Ser^{141},Gly^{149}, Phe^{153}, Pro^{154},Pro^{157},Phe^{168}, Ser^{170}, Asn^{171}, Tyr^{176}, Ile^{178}, Trp^{179} are totally conserved. In the AadA multiple alignment study, we observed that the five stretches PWRYPA, LQFGEW, RIWYS, PKDVAA and ERLPA are highly conserved across species and residues Asp^{49}, Ser^{74}, Pro^{77}, Arg^{84}, Glu^{87}, Thr^{89}, Val^{91}, Arg^{105}, Arg^{114}, Asp^{116}, Ile^{117}, Leu^{118}, Gly^{120}, Phe^{122}, Glu^{123}, Pro^{124}, Asp^{128}, Asp^{130}, Leu^{131}, Ala^{132}, Leu^{134}, Thr^{136}, Lys^{137}, Ala^{138}, Arg^{139}, His^{141}, Ser^{142}, Ala^{144}, Leu^{145}, Gly^{147}, Pro^{148}, Ala^{150}, Phe^{154}, Pro^{156}, Val^{157}, Leu^{166}, Thr^{169}, Trp^{173}, Asn^{174}, Asp^{178}, Trp^{179}, Glu^{183}, Arg^{184}, Asn^{185}, Val^{187}, Leu^{188}, Leu^{190}, Thr^{199}, Gly^{200}, Ile^{202}, Trp^{211}, Pro^{122}, Ala^{227}, Arg^{228}, Ala^{230}, Tyr^{231}, Leu^{232}, Gly^{233}, Asp^{237}, Leu^{239}, Ala^{240}, Arg^{242}, Phe^{249}, Tyr^{252}, Lys^{254} are totally conserved. Among these stretches, the following amino acids in *K. pneumoniae* are involved in hydrogen bonding interactions with the inhibitor: Ser^{32}, Ile^{46}, Glu^{53}, Gln^{54}, Phe^{57}, Thr^{72}, Met^{76}, Val^{78}, Leu^{79}, Ser^{122}, Tyr^{128} and Ile^{151} in case of DHFR (Fig. 6a) and show 100 % conservation against *E. coli* and *Enterobacter cloacae*. For AadA (Fig. 6b), Phe^{34}, Asp^{60}, Arg^{63}, Gln^{64}, Leu^{68}, Glu^{87}, Thr^{89}, Val^{90} show 99 % conservation against *Riemerella anatipestifer*, *Kluyvera intermedia*, *Vibrio cholera*, *E. coli and Achromo bacterxylosoxidans*. The interaction residues were compared with the earlier experimental complex results and interaction coordination was found to closely resemble experimental results [37–40]. The structure of DHFR and AadA has been well characterized in various microorganisms using X-ray crystallography [35, 41]. The results of these studies revealed that, despite considerable structural diversity, all DHFR and AadA monomers share a similar topology and fold. The active site of the enzyme is proposed to be located at the cleft between the N-terminal and C-terminal domains. Conserved residues Leu^{79}, Pro^{80}, Arg^{82}, Val^{87}, Ser^{88}, Lys^{89}, Ser^{122}, Gly^{123}, Gly^{124}, Gly^{125}, Gln^{126}, Ile^{127}, Tyr^{128} and Ile^{15} of DHFR are involved in different types of interaction, viz. hydrogen bond, hydrophobic, cationic, polar, pi-pi and cation-pi interactions with the inhibitor. Lee et al. [35] also reported active sites that are prominently involved in interaction in the crystal structure of DHFR from *Streptococcus pneumoniae*. In AadA, Asn^{59}, Asp^{60}, Arg^{63}, Gln^{64}, Met^{67}, Leu^{68}, Ser^{75}, Pro^{76}, Pro^{77}, Glu^{87}, Leu^{88} and Thr^{89} residues interact with the inhibitor and also found to be highly conserved across the active site stretches of different species. Pedersen et al. [41] reported active site residues in nucleotidyltransferase crystal structure that closely resemble the docking results. Structural analysis and docking investigations of clindamycin with DHFR and AadA suggest that clindamycin will be a better drug for inhibiting these proteins. The best docked protein–ligand complex has been deposited in PMDB. PMDB IDs are PM0078478 and PM0078479 for clindamycin with DHFR and clindamycin with AadA complexes, respectively.

In the DHFR domain of *K. pneumoniae*, Ile^{31}, Ile^{40}, Ile^{46}, Phe^{57} and Met^{76} residues are involved in hydrophobic interactions; Ile^{40}, Ser^{122} residues are involved in hydrogen bonding; Gln^{54}, Ser^{122} and Tyr^{128} in polarization and Phe^{57} in a cation-pi interaction with clindamycin. The estimated free energy of binding was −4.71 kcal/mol with estimated inhibition constant 350.54 μM and an interacting surface area of 577.539 for DHFR. In the case of AadA, Thr^{89} is involved in hydrogen bonding; Glu^{87} and Thr^{89} in polarization; while Phe^{34}, Leu^{51}, Pro^{98} and Asp^{60} are involved in hydrophobic and halogen bonding. Docking of clindamycin with AadA resulted in an estimated free energy of binding of −5.87 kcal/mol with estimated inhibition constant 49.90 μM and interacting surface area of 649.001. This docking study suggests that clindamycin inhibits functionally active domain of both DHFR and AadA proteins of *K. pneumoniae* with lowest energy and highest affinity.

Conclusions

The prevalence of MDR *K. pneumoniae* is alarmingly high in diabetic foot patients in India because of the indiscriminate use of antibiotics. In this study, we characterized the genetic basis of the MDR phenotype in *K. pneumoniae* in relation to its class 1 integron. To the best of our knowledge, this is the first study to report modeling of DHFR and AadA enzymes and their docking with target drugs and inhibitors. The study identifies amino acid residues crucial to 'DHFR and AadA-drug' and 'DHFR and AadA -inhibitor' interactions. An understanding of the residues involved in inhibition with clindamycin could provide useful insights into the identification of new antibacterial compounds and also help in the design of new inhibitors.

Acknowledgments S.K.S. is grateful to the Indian Council of Medical Research, New Delhi (India), for the award of Senior Research Fellowship (80/622/2009-ECD-1). This work is partially supported by a research grant sanctioned to A.K. by the Indian Agricultural Research Institute (No. NBAIM/AMAAS/MD (19)/AK/BG), New Delhi. The facilities provided by Department of Biotechnology (DBT)-funded Sub-Distributed Information Centre (SUB-DIC), Centre for Bioinformatics, School of Biotechnology, Banaras Hindu University (BHU), Varanasi, is gratefully acknowledged.

References

1. Gadepalli R, Dhawan B, Sreenivas V, Kapil A, Ammini AC, Chaudhry R (2006) A clinico-microbiological study of diabetic foot ulcers in an Indian tertiary care hospital. Diabetes Care 29:1727–1732
2. Pinzur MS, Slovenkai MP, Trepman E, Shields NN (2005) Guidelines for diabetic foot care: recommendations endorsed by the diabetes committee of the American orthopaedic foot and ankle society. Foot Ankle Int 26:113–119
3. Lipsky BA, Berendt AR, Deery HG, Embi JM, Joseph WS, Karchmer AW, LeFrock JL, Lew DP, Mader JT, Norden C, Tan JS (2004) Diagnosis and treatment of diabetic foot infections. Clin Infect Diseases 39:885–910

4. Chincholikar DA, Pal RB (2002) Study of fungal and bacterial infections of the diabetic foot. Indian J Pathol Microbiol 45:15–22
5. Umadevi S, Kumar S, Joseph NM, Easow JM, Kandhakumari G, Srirangaraj S, Raj S, Stephen S (2011) Microbiological study of diabetic foot infections. Indian J Med Specialit 2:12–17
6. Kawai T (2006) Hypermucoviscosity: an extremely sticky phenotype of *Klebsiella pneumoniae* associated with emerging destructive tissue abscess syndrome. Clin Infect Dis 42:1359–1361
7. Jones ME, Peters E, Weersink AM, Fluit A, Verhoef J (1997) Widespread occurrence of integrons causing multiple antibiotic resistances in bacteria. Lancet 349:1742–1743
8. El-Najjar NG, Farah MJ, Hashwa FA, Tokajian ST (2010) Antibiotic resistance patterns and sequencing of class I integron from uropathogenic *Escherichia coli* in Lebanon. Lett Appl Microbiol 51:456–461
9. Mazel D (2006) Integrons: agents of bacterial evolution. Nat Rev Microbiol 4:608–620
10. Gebreyes WA, Altier C (2002) Molecular characterization of multidrug-resistant *Salmonella enterica* subsp. *enterica* serovar Typhimurium isolates from swine. J Clin Microbiol 40:2813–2822
11. Holger C, Smith DEC, Blom H, Blau N, Bode H, Holzmann K, Pannicke U, Hopfner KP, Rump EM, Ayric Z, Kohne E, Debatin KM, Smulders Y, Schwarz K (2011) Dihydrofolate reductase deficiency due to a homozygous DHFR mutation causes megaloblastic anemia and cerebral folate deficiency leading to severe neurologic disease. Am Soc Human Genet 88:226–231
12. Schnell JR, Dyson HJ, Wright PE (2004) Structure, dynamics, and catalytic function of dihydrofolate reductase. Annu Rev Biophys Biomol Struct 33:119–140
13. Thomas D, Guenter A, Gerd B, Uwe J, Tarmo P, Robert H, Rainer J (2000) The crystal structure of dihydrofolate reductase from *Thermotoga maritima*: molecular features of thermostability. J Mol Biol 297:659–672
14. Azucena E, Grapsas I, Mobashery S (1997) Properties of a bifunctional bacterial antibiotic resistance enzyme that catalyzes ATP dependent 2″-phosphorylation and acetyl-CoA dependent 6′-acetylation of aminoglycosides. J Am Chem Soc 119:2317–2318
15. Ferretti JJ, Gilmore KS, Courvallin P (1986) Nucleotide sequence analysis of the gene specifying the bifunctional 6′-aminoglycoside acetyltransferase 2″-aminoglycoside phosphotransferase enzyme in *Streptococcus faecalis* and identification and cloning of gene regions specifying the two activities. J Bacteriol 167:631–638
16. Wagner FW (1981) The dysvascular foot: a system for diagnosis and treatment. Foot Ankle 2:64–122
17. Bauer AW, Kirby WM, Sherris JC, Turck M (1966) Antibiotic susceptibility testing by a standardized single disk method. Am J Clin Patholo 45:493–496
18. Clinical and Laboratory Standards Institute (2007) Performance standards for antimicrobial susceptibility testing: Seventeenth informational supplement. Wayne, PA, pp M100–S17
19. Levesque C, Piche L, Larose C, Roy P (1995) PCR mapping of integrons reveals several novel combinations of resistance genes. Antimicrob Agents Chemother 39:185–191
20. Solovyev V, Kosarev P, Seledsov I, Vorobyev D (2006) Automatic annotation of eukaryotic genes, pseudogenes and promoters. Genome Biol 7:1–10
21. Quevillon E, Silventoinen V, Pillai S, Harte N, Mulder N, Apweiler R, Lopez R (2005) InterProScan: protein domains identifier. Nucleic Acids Res 33:116–120
22. Thompson JD, Higgins DG, Gibson TJ (1994) CLUSTAL W: improving the sensitivity of progressive multiple sequence alignment through sequence weighting, position-specific gap penalties and weight matrix choice. Nucleic Acids Res 22:4673–4680
23. Tamura K, Dudley J, Nei M, Kumar S (2007) MEGA4: molecular evolutionary genetics analysis (MEGA) software version 4.0. Molecular Biol Evol 24:1596–1599
24. Bailey TL, Gribskov M (1998) Combining evidence using p-values: application to sequence homology searches. Bioinformatics 14:48–54
25. Bailey TL, Williams N, Misleh C, Li WW (2006) MEME: discovering and analyzing DNA and protein sequence motifs. Nucleic Acids Res 34:369–373
26. Gao YD, Huang JF (2011) An extension strategy of Discovery Studio 2.0 for non-bonded interaction energy automatic calculation at the residue level (in Chinese). Zool Res 32:262–266
27. Arnold K, Bordoli L, Kopp J, Schwede T (2006) The SWISS-MODEL Workspace: a web-based environment for protein structure homology modeling. Bioinformatics 22:195–201
28. Schwede T, Kopp J, Guex N, Peitsch MC (2003) SWISS-MODEL: an automated protein homology-modeling server. Nucleic Acids Res 31:3381–3385
29. Laskowski RA, Chistyakov VV, Thornton JM (2005) D266-8 PDBsum more: new summaries and analyses of the known 3D structures of proteins and nucleic acids. Nucleic Acids Res 33:266–268
30. Maiti R, Van Domselaar GH, Zhang H, Wishart DS (2004) SuperPose: a simple server for sophisticated structural superposition. Nucleic Acids Res 1(2):W590–W594
31. Bikadi Z, Hazai E (2009) Application of the PM6 semi-empirical method to modeling proteins enhances docking accuracy of AutoDock. J Chem Inf 11:1–15
32. Solis FJ, Wets RJB (1981) Minimization by random search techniques. Math Operations Res 6:19–30
33. Morris GM, Goodsell DS, Halliday RS, Huey R, Hart WE, Belew RK, Arthur JO (1998) Automated docking using a Lamarckian genetic algorithm and an empirical binding free energy function. J Comput Chem 19:1639–1662
34. Rice LB, Sahm D, Bonomo RA (2003) Mechanisms of resistance to antibacterial agents. In: Murray PR, Baron EJ, Pfaller MA, Jorgensen JH, Yolken RH (eds) Manual of clinical microbiology, 8th edn. ASM Press, Washington DC, pp 1074–1101
35. Lee J, Yennawar NH, Gam J, Benkovic SJ (2010) Kinetic and structural characterization of dihydrofolate reductase from *Streptococcus pneumoniae*. Biochemistry 49:195–206
36. She Q, Singh RK, Confalonieri F et al. (2007) Crystal structure of a putative nucleotidyltransferase (AAK41883.1) from *Sulfolobus solfataricus* at 1.40 Å resolution. Joint Center for Structural Genomics Submitted to the PDB data bank, doi:10.2210/pdb2rff/pdb
37. Feeney J, Birdsall B, Kovalevskaya NV, Smurnyy YD, Navarro Peran EM, Polshakov VI (2011) NMR structures of apo *L. casei* dihydrofolate reductase and its complexes with trimethoprim and NADPH: contributions to positive cooperative binding from ligand-induced refolding, conformational changes, and interligand hydrophobic interactions. Biochemistry 50:3609–3620
38. Cody V, Galitsky N, Rak D, Luft JR, Pangborn W, Queener SF (1999) Ligand-induced conformational changes in the crystal structures of *Pneumocystis carinii* dihydrofolate reductase complexes with folate and $NADP^+$. Biochemistry 38:4303–4312
39. Gargaro AR, Soteriou A, Frenkiel TA, Bauer CJ, Birdsall B, Polshakov VI, Barsukov IL, Roberts GC, Feeney J (1998) The solution structure of the complex of *Lactobacillus casei* dihydrofolate reductase with methotrexate. J Mol Biol 20:119–134
40. Vidya N, Vadivukkarasi B, Manivannan G, Anbarasu K (2008) Molecular modeling and docking studies of glutamate racemase in *Vibrio vulnificus* CMCP6. Silico Biol 8:471–483
41. Pedersen LC, Benning MM, Holden HM (1995) Structural investigation of the antibiotic and ATP-binding sites in kanamycin nucleotidyltransferase. Biochemistry 34:13305–13311